

A Single Channel GLR Detector for High-Frequency Surface Wave Radar

M. R. Moniri, M. Nezamabadi

Yadegar-e-Imam Khomeini (RAH) Shahre Rey Branch, Islamic Azad University
Tehran, Iran

Abstract— There are various interference sources in the environment of high frequency surface wave radar (HFSWR) which limit detection of small targets. In the work presented here, single-sensor AR-GC-GLR detector examined for actual sea clutter gathered by a HFSWR. Using simulation and practical measurements, the performance of this detector will be proposed. Findings show that the performance of detection will improve by fewer numbers of the interference samples. This dependency is more than ground clutter with sparse plant coverage, which is considered as AR-GC-GLR detector.

Keywords— *Single Channel; HFSWR; Autoregressive process; Gaussian Spectrum*

I. INTRODUCTION

HFSWR which operates at 3-15MHz, has the ability to detect and track surface and airborne targets in real time and over the horizon by surface wave propagation in addition to normal line-of-sight propagation at the distance of up to 300Km [1], [2]. HFSWR is classified into onshore and ship borne HFSWR but we didn't address the later type of HFSWR.

Signal detection is an important component in HFSWR designing. The detection performance is limited by presence of clutter and interference signals that are not stationary. Also, at the S-band (2-4GHz) marine radar, the size of range cells are in meters order and targets such as ships, take several cells of this magnitude, so that the signal to clutter ratio (SCR) can attain suitable value. However, with HFSWR, taking the several hundred ranges and broad beam width into account, the long pulse width is used to obtain the desired gain. Typical size of range cell in HFSWR is 1.5 to 4-5km. So, the SCR is too small to detect targets. In addition, the detection of low speed targets whose Doppler frequency of them is close to Bragg lines of sea clutter, is too difficult.

Several attempts have been made to overcome mentioned problems. It is effectiveness to use adaptive processing in these conditions. Abramovich et al. [3, 4] considered spatio-temporal adaptive array processing in OTHR (over-the horizon radar) and airborne radar applications to remove non-stationary multipath interference (hot clutter). He used "stochastic constraints" to achieve effective hot clutter suppression

while maintaining distortionless output cold clutter (sea/terrain signal) post processing stationary. Fabrizio et al. [5] proposed a computationally effective TV (time-varying) fast-time STAP (space-time adaptive processing) algorithm that can effectively cancel hot clutter during the CPI (coherent processing interval) while simultaneously preserving the Doppler spectrum characteristics of cold clutter. Fabrizio et al. [6] focused on HFSWR and presented an adaptive beamformer that effectively suppresses non-stationary interference without degrading SCV (sub-clutter visibility). Saleh [7] studied the use of STAP algorithms [8 - 11] and applied them to HFSWR.

In addition, Ravan et al. [12] addressed the detection of small vessels in the presence of highly nonhomogeneous sea clutter based on developed FFA (fast fully adaptive) approach that is two-stage STAP algorithm. In [13, 14] attempted to prove JDL (Joint Domain Localized) to be effective algorithm for ionospheric clutter suppression for HFSWR.

For detecting weak targets masked by nonhomogeneous ionospheric clutter, Zheng et al. [15] used an algorithm based on angle-Doppler joint eigenvector which considers the angle-Doppler map of radar echoes is adopted to analyze the characteristics of the nonhomogeneous ionospheric clutter.

Another approach is using detection theory and Fabrizio et al. [16] proposed a GLRT (generalized likelihood ratio test) based adaptive Doppler processing method for ship detection with short CPI in HFSWR. It possess the valuable CFAR (constant false alarm rate) property invariant and has distinct advantages over the ACE (adaptive coherence estimator) [18] and ASD (adaptive subspace detector) [20] for HFSWR.

Sheikhi et al. [19] modeled the interference with AR (Auto-Regressive) process proposed for single-sensor radar. Moniri et al. [20] extended to multi-channel and called it as "M-AR-GC-GLR" (Multi channel Auto-Regressive Gaussian spectrum Generalized Likelihood Ratio). In the case of single-sensor and considering Gaussian shape for correlation function of interference, Moniri et al. [21] presented "AR-GC-GLR" detector for airborne radar to detect targets with known Doppler and unknown complex amplitude in the complex

Gaussian noise environment with unknown parameters.

With respect to superiority of AR-GC-GLR to the AR-GLR and Kelly's GLR detectors [21], in the present study, we applied the AR-GC-GLR for HFSWR application and used real sea clutter data to examine the performance of it.

II. AR-GC-GLR

All notations used are the same [21]. We assume that the discrete complex process $\underline{y}(k)$ received by a single-sensor pulsed radar system. Thus, the detection problem is given by:

$$\begin{aligned} H_0: \underline{y}(0) = \underline{n}(0) \\ \underline{y}(k) = \underline{n}(k) \quad (k = 1, 2, \dots, K) \\ H_1: \underline{y}(0) = \underline{n}(0) + \underline{a}\underline{s} \\ \underline{y}(k) = \underline{n}(k) \quad (k = 1, 2, \dots, K) \end{aligned} \quad (1)$$

so, $\underline{y}(k)$ is a complex N-dimensional vector (corresponding to N-pulse train) and $\underline{y}(0)$ represents the primary data received from the cell under test for absence of the H_0 hypothesis and for H_1 hypothesis the target signal \underline{s} is added. For $k = 1, 2, \dots, K$ they are secondary data which are iid and include no target for both hypothesis. \underline{s} is also a complex N-dimensional vector which denotes the target signal and is given by:

$$\underline{s} = [s_1 \ s_2 \ \dots \ s_N]^T = [1 \ e^{j\Omega} \ \dots \ e^{j(N-1)\Omega}]^T \quad (2)$$

where T stands for transpose. This vector corresponds to a target whose Doppler is Ω , which is assumed to be known. α is an unknown complex amplitude of reflected signal from the target. $\underline{n}(k)$ is also a complex N-dimensional vector denoting the clutter:

$$\underline{n}(k) = [n_{k,1} \ n_{k,2} \ \dots \ n_{k,N}]^T \quad (3)$$

which is assumed to be an Auto-Regressive (AR) process of order M with parameters \underline{a} and σ_u^2 , $AR(M, \underline{a}, \sigma_u^2)$, σ_u^2 is variance of zero-mean discrete complex white Gaussian noise and $\underline{a} = [a_1 \ a_2 \ \dots \ a_M]$ is the AR parameter vector. We assume that \underline{a} and σ_u^2 are also unknown but \underline{a} can be expressed in terms of other unknown parameters. We use Gaussian correlation function

$$R(l) = \sigma^2 (\lambda)^{|l|} \quad (4)$$

that is suitable model for our measurements.

The quantity λ is defined as temporal correlation parameter, which provides a measure for the correlation between samples of the process and is a real parameter such that $\lambda \in [0,1]$. Now, the Yule - Walker equations can be used to determine the AR coefficients of the process. For second order (M=2) AR process $\underline{a}(\lambda)$ is given by:

$$\underline{a}(\lambda) = [-\lambda(\lambda^2 + 1) \ \lambda^2]^T \quad (5)$$

$$\sigma^2 = \frac{\sigma_u^2}{1 - \lambda^2 - \lambda^4 + \lambda^6} \quad (6)$$

Now, we discuss the detection problem which is expressed as Eq. (1). The GLR theory can then be applied here. The resulting detector compares the likelihood ratio, L_{GLR} , with a threshold η .

$$\begin{aligned} L_{GLR} &= \frac{\max_{\sigma_u^2, \lambda, \alpha} f_Y(\underline{y}(0), \underline{y}(1), \dots, \underline{y}(K)) | H_1, \sigma_u^2, \lambda, \alpha)}{\max_{\sigma_u^2, \lambda} f_Y(\underline{y}(0), \underline{y}(1), \dots, \underline{y}(K)) | H_0, \sigma_u^2, \lambda, \alpha = 0} \\ &= \frac{f_Y(\underline{y}(0), \underline{y}(1), \dots, \underline{y}(K)) | H_1, \hat{\sigma}_{u1}^2, \hat{\lambda}_1, \hat{\alpha}}{f_Y(\underline{y}(0), \underline{y}(1), \dots, \underline{y}(K)) | H_0, \hat{\sigma}_{u0}^2, \hat{\lambda}_0, \alpha = 0} \Bigg|_{H_0} \eta \end{aligned} \quad (7)$$

Since $\underline{n}(k)$ is assumed to be Gaussian, we have:

$$\begin{aligned} f_i &= f_Y(\underline{y}(0), \underline{y}(1), \dots, \underline{y}(K)) | H_1, \sigma_u^2, \lambda, \alpha \\ &\equiv \left(\frac{1}{\pi^N \sigma_u^{2N}} \right)^{K+1} \prod_{k=0}^K \exp \left(-\frac{1}{\sigma_u^2} \sum_{n=M+1}^N \left| x_{k,n} - \sum_{j=1}^M a_j(\lambda) x_{k,n-j} \right|^2 \right) \end{aligned} \quad (8)$$

where $x_{0,n} = y_{0,n} - \alpha s_n$ and $x_{k,n} = y_{k,n}$ for $k=1, 2 \dots K$ and for f_0 we have:

$$\begin{aligned} f_0 &= f_Y(\underline{y}(0), \underline{y}(1), \dots, \underline{y}(K)) | H_0, \sigma_u^2, \lambda, \alpha = 0 \\ &\equiv \left(\frac{1}{\pi^N \sigma_u^{2N}} \right)^{K+1} \prod_{k=0}^K \exp \left(-\frac{1}{\sigma_u^2} \sum_{n=M+1}^N \left| y_{k,n} - \sum_{j=1}^M a_j(\lambda) y_{k,n-j} \right|^2 \right) \end{aligned} \quad (9)$$

By using Eq. (8) and Eq. (9) in Eq. (7), the detector is derived and given by:

$$\ln L_{GLR} = N(K+1) \left(\ln(\hat{\sigma}_{u1}^2) - \ln(\hat{\sigma}_{u0}^2) \right) \eta \quad (10)$$

where:

$$\hat{\sigma}_{u0}^2 = \frac{1}{N(K+1)} (\underline{u} \ \underline{Y} \underline{a}(\hat{\lambda}_0))^H (\underline{u} \ \underline{Y} \underline{a}(\hat{\lambda}_0)) \quad (11)$$

$$\underline{Y} = \begin{bmatrix} \underline{y}_0^T & \underline{y}_1^T & \dots & \underline{y}_K^T \\ \underline{y}_1^T & \underline{y}_2^T & \dots & \underline{y}_3^T \\ \vdots & \vdots & \ddots & \vdots \\ \underline{y}_{K-1}^T & \underline{y}_K^T & \dots & \underline{y}_{K+1}^T \end{bmatrix} \quad (12)$$

$$\underline{u} = [\underline{u}_0^T \ \underline{u}_1^T \ \dots \ \underline{u}_K^T]^T, \underline{u}_i = [y_{i,M+1} \ \dots \ y_{i,N}]$$

On the other hand:

$$\hat{\sigma}_{u1}^2 = \frac{1}{N(K+1)} (\underline{u}' - \underline{Y}' \underline{a}(\hat{\lambda}_1))^H (\underline{u}' - \underline{Y}' \underline{a}(\hat{\lambda}_1)) \quad (13)$$

$$(14)$$

$$\underline{Y}' = [\underline{Y}'_0 \quad \underline{Y}'_1 \quad \dots \quad \underline{Y}'_K]^T, \underline{Y}'_0 = \underline{H}\underline{Y}_0$$

$$\underline{u}' = [\underline{u}'_0^T \quad \underline{u}'_1^T \quad \dots \quad \underline{u}'_K^T]^T, \underline{u}'_0 = \underline{H}\underline{u}_0$$

Y_i and u_i are defined in Eq. (12) and H is defined as:

$$H = I - \frac{\Phi\Phi^H}{\Phi^H\Phi} \quad (15)$$

$$\Phi = [1 \quad e^{j\Omega} \quad \dots \quad e^{j(N-M-1)\Omega}] \quad (16)$$

which is the projection matrix of the null space of Φ .

The structure of detector is shown in Fig.1.

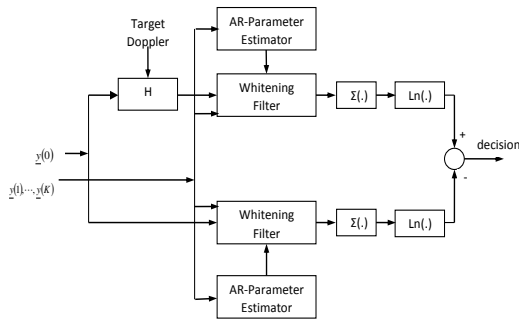


Fig. 1: The AR-GC-GLR block diagram [21]

III. EXPERIMENTAL RESULTS

The sea clutter can be modeled with AR process in order of 2 [5]. We apply the AR-GC-GLR detector for sea clutter that is gathered by an HFSWR. This is a phased array radar and operates at lower half of the HF band. The sampling frequency is 5Hz.

Fig.2 demonstrates a comparison with Kelly's GLR and AR-GLRs detectors as probability of detection (P_d) versus probability of false alarm (P_{fa}). We can see high superiority of AR-GC-GLR. This superiority is the result of using a prior knowledge of being Autoregressive with a Gaussian correlation function in clutter modeling. But Kelly's GLR and AR-GLR don't use this information, so they have a poor performance as compared with AR-GC-GLR [21].

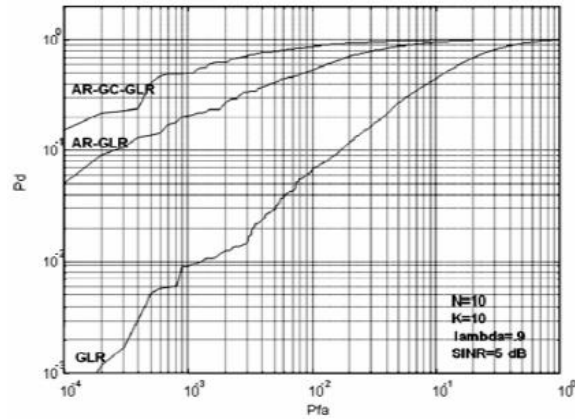


Fig. 2: Comparison with Kelly's GLR and AR-GLR ($\lambda=0.9$) [21]

Fig.3 illustrates the improvement of the detection performance by increasing the temporal correlation parameter (λ) that is because of the chance of the detector to have a better estimation of the clutter behaviors when we have more correlation in our samples. Fig.4 shows the results with real sea clutter data. $\lambda=0.98$, the performance of the detector (i.e. P_d) is approximately 1.

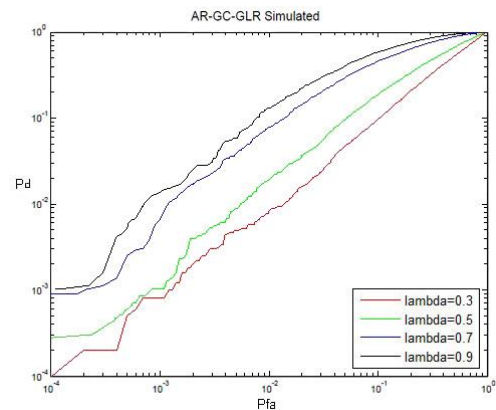


Fig. 3: P_d versus P_{fa} for various temporal correlation parameter (computer simulation): $\lambda=0.4, 0.7, 0.9$

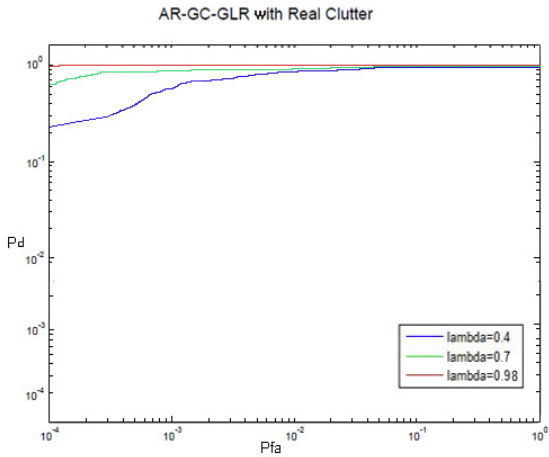


Fig 4: P_d versus P_{fa} for various temporal correlation parameter (real clutter): $\lambda=0.4, 0.7, 0.9$

Fig.5 and Fig.6 show the AR-GC-GLR performance in comparison with AR-GLR against measured clutters. The measured clutter is a result of several measurements on the clutter by an X band radar with pulse duration of 300ns for 15000 samples in each experiments [21]. We did this investigation with real sea clutter measured by HFSWR and shown in Fig.7. As it can be seen, there is significant correlation between the samples of sea clutter that is similar to Ground sparse plant coverage clutter. At both Fig.5 and Fig.7 the performance of detector is very close to 1.

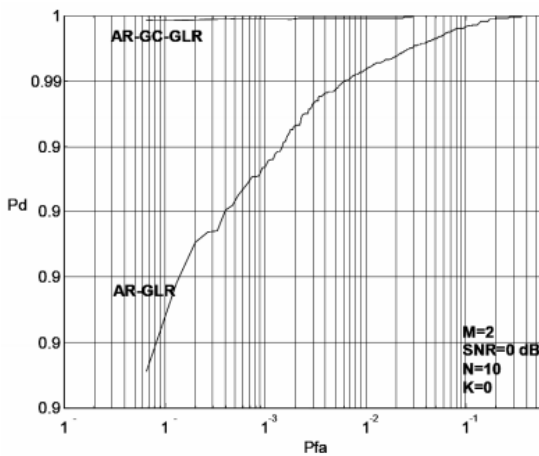


Fig 5: Comparison against AR-GLR: Ground sparse plant coverage, Range 2750 meters [21]

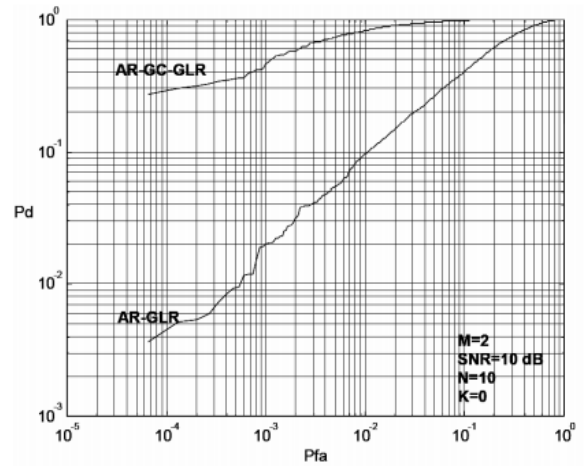


Fig 6: Comparison against AR-GLR: Rain Clutter, Range 320 meters [21]

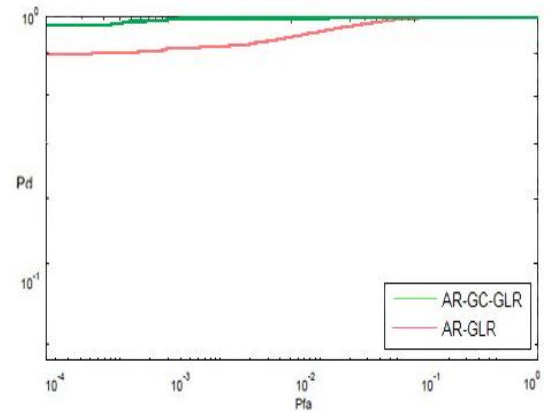


Fig 7: Comparison against AR-GLR: Real Sea clutter

The dependency of the detection performance to the secondary data is depicted in Fig.8. The performance is improved as more secondary data used. As shown in Fig.9 for real sea clutter data, when the number of secondary data increases, we observe different result and the performance of detector is degraded.

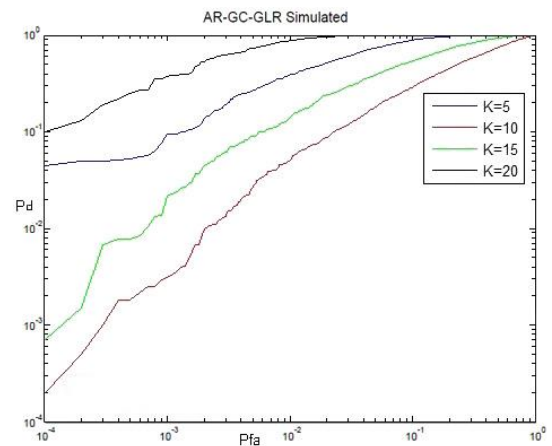


Fig. 8: P_d versus P_{fa} for various number of secondary data (computer simulation)

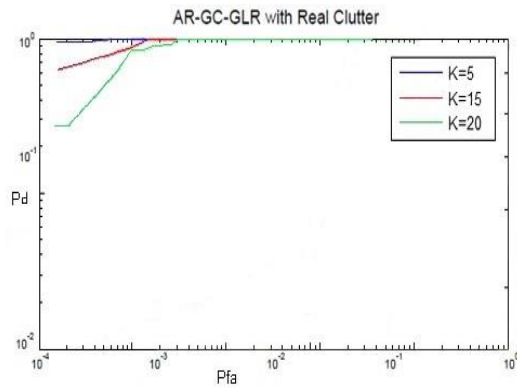


Fig. 9: P_d versus P_{fa} for various number of secondary data (real clutter)

Performance improvement by increasing observations in time are demonstrated in fig. 10 and fig. 11.

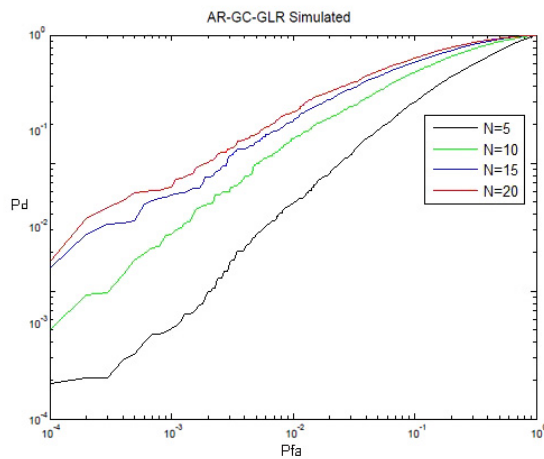


Fig. 10: P_d versus P_{fa} for various number of pulses (computer simulation)

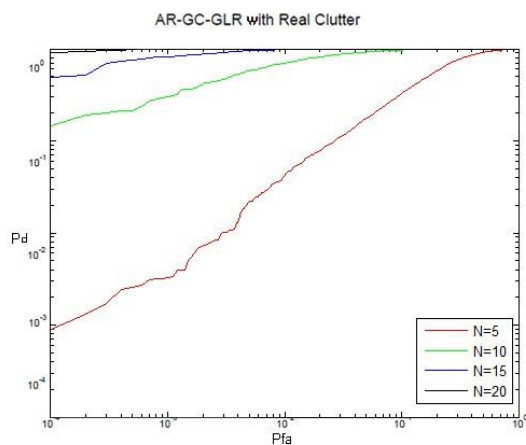


Fig. 11: P_d versus P_{fa} for various number of pulses (real clutter)

IV. CONCLUSION

We applied THE AR-GC-GLR detector, considering one sensor of HFSWR and examined its performance through computer simulations, as well as real data clutter.

It seemed liked that the temporal correlation of sea clutter samples was considerably higher than the ground clutter with sparse plant and rain clutter that was considered in [10] and caused improvement to the performance of AR-GC-GLR detector. In HFSWR applications, numerous secondary data lead to degradation of performance of detector. With large range cells at HFSWR, by the increase in the number of secondary data, we may meet the edge of clutter, or stormy weather or a ship that may destroy the uniform structure of the clutter. Also, when considering one sensor of antenna, with respect to large range cells, we may meet a ring of clutter that the sea waves may develop positive Doppler at part of this ring, while another having negative or zero Doppler at other parts. Hence the uniform structure of the clutter may be destroyed. But we tend to consider a uniform structure for the clutter. As a result, the CFAR property of detector will be lost. There is no real single channel of HFSWR. So, it is suggested that the multi-channel version of this algorithm is studied with HFSWR.

ACKNOWLEDGMENT

The authors are thankful to JMEST Journal for the support to develop this document.

REFERENCES

- [1] L. Sevgi, A. Ponsford, H. C. Chan, "An integrated maritime surveillance system based on high-frequency surface-wave radars, part 1:theoretical background and numerical simulations", IEEE Antennas and propagation Magazine, vol. 43, no. 5, pp. 28-43, October 2001
- [2] A. Ponsford, L. Sevgi, H. C. Chan, "An integrated maritime surveillance system based on high-frequency surface-wave radars, part 2:Operational status and system performance", IEEE Antennas and propagation Magazine, vol. 43, no. 5, pp. 52-63, October 2001
- [3] Y. I., Abramovich, N. K., Spencer, S. J., Anderson, A. Y., Gorokhov, "Stochastic-Constraints Method in Nonstationary Hot-clutter Cancellation-PartI: Fundamentals and Supervised Training Applications", IEEE Transactions on Aerospace and Electronic Systems, vol. 34, no. 4, pp.1271-1292, October 1998
- [4] Y. I., Abramovich, N. K., Spencer, S. J., Anderson, "Stochastic-Constraints Method in Nonstationary Hot-clutter Cancellation-PartII: Unsupervised Training Applications", IEEE Transactions on Aerospace and Electronic Systems, vol. 36, no. 1,pp. 132-150, Jan 2000
- [5] A. G. Fabrizio, A. Farina, "Time-Varying STAP for Nonstationary Hot Clutter Cancellation", IEEE International Conference on Acoustic, Speech and Signal Processing(ICASSP), May 2014
- [6] A. G. Fabrizio, A. B. Gersham, M. D. Turley, "Non-Stationary Interference Cancellation in HF Surface

- Wave Radar”, Proc of IEEE Radar Conference, pp. 672-677, September 2003
- [7] O. Saleh, “Adaptive Processing in High-Frequency Surface WAVE RADAR”, Thesis of Master of Applied Science, University of Toronto, 2008
- [8] R. Adve, T. Hale, and M. Wicks, April 2000, “Joint domain localized adaptive processing in homogeneous and non-homogeneous environments part I: Homogeneous environments”, IEE Proc of Radar, Sonar Navigation, vol. 147, No. 2, pp. 57-65, 2007
- [9] J. E. Yang, J. Chun, and R. Adve, “A hybrid D3-Sigma Delta STAP algorithm in non-homogeneous clutter”, IET International Conference On Radar Systems, October 2007
- [10] J. Roman, M. Rangaswamy, D. Davis, Q. Zhang, B. Himed, J. Michels, “Parametric adaptive matched filter for airborne radar applications,” IEEE Transactions on Aerospace and Electronic Systems, vol. 36, no. 2, pp. 677-692, 2000
- [11] J. Goldstein, I. Reed, and L. Scharf, “A Multistage Representation of the Wiener Filter Based on Orthogonal Projections,” IEEE Transactions on Information Theory, vol. 44, no. 7, pp. 2943-2959, 1998
- [12] M. Ravan, R. S. Adve, “Robust STAP for HFSWR in dense target scenarios with nonhomogeneous clutter”, IEE Radar Conference, May 2012
- [13] X. Zhang, Q. Yang, Ch. Zhang, W. Deng, “Post-DBF joint domain localized rapid parallel implementation for HFSWR based on GPU”, IET Radar Conference, October 2015
- [14] X. Zhang, W. Deng, Q. Yang, Y. Dong, “Modified Space-Time Adaptive Processing with first-order bragg lines kept in HFSWR”, IEEE International Radar Conference, October 2014
- [15] X. Zhang, Q. Yang, W. Deng, “Weak Target Detection within the NonHomogeneous Ionospheric Clutter Background of HFSWR Based on STAP”, International Journal of Antennas and Propagation, Article ID:382516, 11 pages, 2013
- [16] A. G. Fabrizio, A. Farina, “GLRT-Based Adaptive Doppler Processing for HF Radars Systems”, IEEE International conference, Acoustic, Speech and Signal Processing (ICASSP), pp. II949 – II952, April 2007
- [17] L. L. Scharf, L. T. Mc Whorter, “Adaptive Matched Subspace Detectors and Adaptive Coherence”, Proc of 30th Asilomar Conference on Signals, Systems and Computers, Pacific Grove, Calif., US, 1996
- [18] S. Kraut, L. L. Scharf, “The CFAR Adaptive Subspace Detector is a Scale-invariant GLRT”, IEEE Transactions on Signal Processing, vol. 47, no. 8, pp. 2538-2541, 1999
- [19] A. Sheikhi, M. M. Nayebi, M. R. Aref, “Adaptive Detection Algorithm for Radar Signals in Autoregressive interference”, IEE Proc of Radar, Sonar Navigation, vol. 145, no. 5, 309-314, October 1998
- [20] M. R. Moniri, M. M. Nayebi, A. Sheikhi, “A Multichannel Auto-Regressive GLR Detector for Airborne Phased Array Radar application”, IEE Proc of Radar, Sonar Navigation Conference, pp. 206-211, September 2003
- [21] M. R. Moniri, M. M. Nayebi, A. Sheikhi, “Adaptive Signal Detection in Auto-Regressive Interference with Gaussian Spectrum”, Iranian Journal of Electrical & Electronic Engineering, vol. 4, no. 4, pp.144-149, 2008